A&A 389, 202–212 (2002)
DOI: 10.1051/0004-6361:20020506

Astronomy & Astrophysics

Doppler imaging of stellar surface structure

XVIII. The very active RS CVn binary UZ Librae revisited

K. Oláh[1], K. G. Strassmeier[2,⋆,⋆⋆], and M. Weber[2,⋆]

[1] Konkoly Observatory of the Hungarian Academy of Sciences, 1525 Budapest, Hungary
e-mail: olah@konkoly.hu
[2] Astrophysical Institute Potsdam (AIP), An der Sternwarte 16, 14482 Potsdam, Germany

Received 7 December 2001 / Accepted 3 April 2002

Abstract. We present eight Doppler images of UZ Librae from the years 1994, 1996, 1997, 1998 and 2000. These maps indicate a preferred temperature distribution from one year to the other and suggest preferred spot locations for at least the seven years of our observations. Two equatorial active regions appear facing towards and opposite the (unseen) companion star. A large and cool polar spot, with two or maybe three appendages extending down to a latitude of 40°–50°, is present and causes the long-term light variability of UZ Lib. The appendages appear at longitudes very similar to the two equatorial active regions and sometimes are possibly even attached to them. No coherent sign of differential rotation is found for the equatorial regions up to a latitude of approximately +50°, but the polar appendages may indicate a general acceleration of the polar regions. If interpreted as being due to differential rotation, if real at all, then UZ Lib clearly exhibits a non-solar flow pattern.

Key words. starspots – stars: activity – stars: atmospheres – stars: late-type – stars: individual: UZ Lib – stars: binaries: close

1. Introduction

The first paper of this series on *Doppler Imaging of stellar surface structure* was published six years ago on the active giant UZ Librae (Strassmeier 1996). In that paper the history of the literature on UZ Librae is summarized and the problems relating to its basic astrophysical properties are discussed in some detail. An update of the observations available since then, especially regarding the distance, is given in Fekel et al. (1999) and in a recent paper by Oláh et al. (2002a) on the photometric behavior of UZ Librae.

UZ Lib is the giant primary of a close binary system with extremely fast rotation and revolution and is one of the most active RS CVn binaries in the sky (Bopp & Stencel 1981). The rotational and orbital period is only 4.76 days. Modelling photometric data taken between 1993–2001, Oláh et al. (2002a,b) found a surprisingly well-defined phase coherence of the light-curve minima for eight consecutive years. If interpreted as being due to spots, two main spotted regions centered at approximately 90° and 270° longitude were possibly present at all times. In the same paper, the authors found evidence for a long-term trend of the overall system brightness with a possible cycle period of about 5.4 years. In this paper, we present Doppler images of UZ Lib for the years 1994, 1996, 1997, 1998 and 2000, of which the 1994 data is that from Strassmeier (1996). Thus, all our spectroscopic data on UZ Lib is treated in a uniform manner.

2. Observations

2.1. High-resolution spectroscopy

A total of 68 spectra were obtained with the 0.9-m coudé-feed telescope at Kitt Peak National Observatory (KPNO) between 1994 and 2000. The observing log in Table 1 summarizes their time and phase distribution and gives information on the data content of the individual Doppler images. Details of the 1994 data were given in Strassmeier (1996). The new KPNO data from 1996 to 2000 were obtained with the same spectrograph setup as in 1994, i.e. grating A, camera 5 and the long collimator but with the higher-efficiency 3096 × 1024 CCD (F3KB chip, 15μ pixels). An example of the full spectrum of UZ Lib was plotted in Fig. 1 in Fekel et al. (1999). The effective resolution with the F3KB CCD was 27 000 (11 km s^{-1}) as

Send offprint requests to: K. G. Strassmeier,
e-mail: Kstrassmeier@aip.de, Mweber@aip.de
⋆ Visiting Astronomer, Kitt Peak National Observatory, operated by the Association of Universities for Research in Astronomy, Inc. under contract with the National Science Foundation.
⋆⋆ ESO visiting astronomer.

Table 1. Spectroscopic log.

HJD	orb.phase	telescope	dataset
2449417.0161	0.0653	KPNO	1994
2449418.0131	0.2744	KPNO	
2449420.9964	0.9000	KPNO	
2449422.0139	0.1134	KPNO	
2449423.0166	0.3237	KPNO	
2449424.0096	0.5318	KPNO	
2449424.9628	0.7319	KPNO	
2449426.0109	0.9517	KPNO	
2449427.0074	0.1607	KPNO	
2449428.0097	0.3709	KPNO	
2449429.0005	0.5787	KPNO	
2449429.9114	0.7697	KPNO	
2450096.0289	0.4685	KPNO	1996
2450097.0354	0.6796	KPNO	
2450098.0336	0.8889	KPNO	
2450099.0368	0.0993	KPNO	
2450101.0372	0.5188	KPNO	
2450102.0373	0.7286	KPNO	
2450103.0370	0.9382	KPNO	
2450104.0397	0.1485	KPNO	
2450107.0329	0.7763	KPNO	
2450108.0406	0.9876	KPNO	
2450221.5782	0.7988	ESO	1996-ESO
2450221.8266	0.8509	ESO	
2450222.5811	0.0091	ESO	
2450222.8143	0.0580	ESO	
2450223.5749	0.2176	ESO	
2450224.5995	0.4324	ESO	
2450225.6242	0.6473	ESO	
2450226.5449	0.8404	ESO	
2450226.8130	0.8966	ESO	
2450544.9558	0.6178	KPNO	1997
2450545.9546	0.8273	KPNO	
2450546.9447	0.0350	KPNO	
2450547.9484	0.2455	KPNO	
2450548.9556	0.4567	KPNO	
2450549.9435	0.6639	KPNO	
2450550.9444	0.8738	KPNO	
2450551.9483	0.0843	KPNO	
2450552.8741	0.2785	KPNO	
2450553.8645	0.4862	KPNO	
2450554.8959	0.7025	KPNO	
2450904.9244	0.1108	KPNO	1998a
2450906.8952	0.5241	KPNO	
2450907.8865	0.7320	KPNO	
2450908.8953	0.9436	KPNO	
2450910.8457	0.3526	KPNO	
2450911.8643	0.5663	KPNO	
2450912.8715	0.7775	KPNO	
2450913.8709	0.9871	KPNO*	1998b
2450914.9035	0.2036	KPNO*	
2450916.8698	0.6160	KPNO	
2450917.8705	0.8259	KPNO	
2450920.8735	0.4557	KPNO	
2450921.9393	0.6792	KPNO	
2450922.9092	0.8826	KPNO	
2450923.8570	0.0814	KPNO	
2450924.8996	0.3000	KPNO	

Table 1. continued.

HJD	orb.phase	telescope	dataset
2451636.9655	0.6352	KPNO	2000a
2451637.9766	0.8472	KPNO	
2451638.9707	0.0557	KPNO	
2451640.0063	0.2729	KPNO	
2451640.9992	0.4811	KPNO	
2451641.9761	0.6860	KPNO	
2451642.9991	0.9005	KPNO	
2451644.8988	0.2989	KPNO	
2451660.9258	0.6601	KPNO	2000b
2451661.9155	0.8677	KPNO	
2451662.9186	0.0781	KPNO	
2451663.9521	0.2948	KPNO	
2451664.9380	0.5016	KPNO	
2451665.9625	0.7164	KPNO	
2451666.9136	0.9159	KPNO	
2451667.9636	0.1361	KPNO	
2451668.9615	0.3454	KPNO	

* Used both for the 1998a and 1998b images.

Table 2. Basic data and proxies for UZ Lib.

Parameter	Value	Ref.
Classification	K0(III)	1.
Period, $P_{\rm rot} = P_{\rm orb}$	4.768241 days $\pm$0.000026	2., 3.
$v \sin i$	67 ± 1 km s^{-1}	2., 3.
$T_{\rm eff}$	4800 K	3.
$\log g$	2.5	2.
Inclination, i	$\approx 50^\circ \pm 10^\circ$	
Microturbulence for Ca, $\xi_{\rm Ca}$	0.8 km s^{-1}	
Microturbulence for Fe, $\xi_{\rm Fe}$	0.8 km s^{-1}	
Macroturbulence, $\zeta_{\rm R} = \zeta_{\rm T}$	4.0 km s^{-1}	
Chemical abundance	solar (adopted)	

1. Bopp & Stencel (1981), 2. Strassmeier (1996), 3. Fekel et al. (1999).

compared to 38 000 (8 km s^{-1}) with the TI-5 CCD. With the former, we achieved signal-to-noise (S/N) ratios of about 200:1 in one hour integration time. Additionally to the 68 KPNO spectra, 9 spectra from ESO were obtained in May 1996. The 1.4-m coudé auxiliary telescope (CAT) was used with the coudé echelle spectrograph (CES) in single-order mode. Together with the Loral 2688×512 CCD (15 μm pixels) the spectrograph provided a resolution of 70 000 (4 km s^{-1}). All spectra were centered at around 6430 Å. Data reduction of both the KPNO and the ESO data was performed with the IRAF package and included the standard tasks of bias subtraction, flat-field division, (optimal) aperture extraction, and cosmic-ray clipping. Special attention was paid to the long- and short-term stability of the flat field spectra but even forty flat fields per night did not show any recognizable differences and average flats were used. Continuum setting was performed with a second-order polynomial.

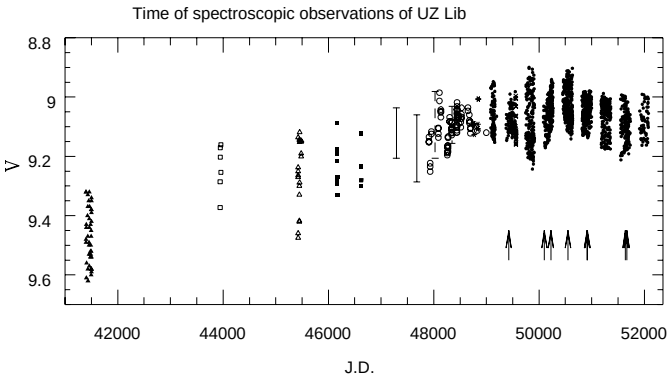

Fig. 1. Long-term photometric brightness changes of UZ Librae from 1972 until 2001. The arrows indicate the times of our spectroscopic observations for Doppler imaging. Note that all spectra were taken during high system brightness. Various symbols denote different data sources from the literature as explained in Oláh et al. (2002a). The dots are APT data.

2.2. Automated photometry

The contemporaneous and partly simultaneous photometric data in this paper were obtained with the two Vienna automatic photoelectric telescopes (APTs; dubbed "Wolfgang" and "Amadeus") at Fairborn Observatory in southern Arizona (Strassmeier et al. 1997b). The Wolfgang data were taken in and transformed to the Strömgren b and y system while the Amadeus data were taken in and transformed to the Johnson-$V(RI)_{\rm C}$ system. The combined $V + y$ data is plotted, among others, in Fig. 1. Part of the early data were already used in the study of Strassmeier et al. (1997a) and later updated in Strassmeier et al. (1999). These papers also include a more detailed description of the observing schedule of the two APTs.

3. Doppler images for 1994–2000

The 68 spectra allowed a total of eight images. According to the Julian dates in Table 1, one image in 1994 and 1997, and two images in 1996, in 1998, and in 2000 were obtained. We repeated the analysis of the original 1994 data first published by Strassmeier (1996). All data sets are supported with simultaneous Johnson V and $I_{\rm C}$ photometry. The two data sets from 2000 are additionally supported with simultaneous Strömgren b and y photometry.

3.1. Method and assumptions

All Doppler maps in this paper were computed with the TempMap code (Rice et al. 1989; Piskunov & Rice 1993; Rice & Strassmeier 2000) using Sun workstations at Konkoly Observatory. TempMap works from a full LTE spectrum synthesis by solving the equation of transfer on 72 depth points of a grid of 10 Kurucz (1993) model atmospheres, and thus also fits the line equivalent width. A total of 2592 surface pixels are included for matching the local effective temperature, for the present case with fixed solar abundances. The code performs simultaneous inversions of all spectral line profiles in a given wavelength region together with two photometric bandpasses. For the UZ Librae spectra, we were able to make use of three main spectral lines including a suite of selected blends: Ca I 6439.076 Å (plus 6 blends), Fe I 6393.602 Å (plus 6 blends) and Fe I 6411.659 Å (plus 5 blends). The transition probabilities of these blends are regularly updated due to ever better atomic data as manifested in the VALD data base (e.g. Stempels et al. 2001). Note that we did not include the Fe I 6430-Å line because it is very strongly blended with the nearby singly-ionized Fe II 6432-Å line that, moreover, contains two extremely temperature-sensitive neutral vanadium lines. See also the brief discussion in Strassmeier & Bartus (2000). We treated the three mapping lines separately, since the spectral coverage our code can handle is currently limited to 2 nm, which is too small for including all the mapping lines at the given $v \sin i$ of UZ Lib (see Rice & Strassmeier 2001) for an application to a different wavelength region).

The basic astrophysical parameters of UZ Librae are summarized in Table 2. The orbital elements in Fekel et al. (1999),

$$\mathrm{HJD} = 2\,449\,993.662 + 4.768241 \times \ E$$

were used for calculating the phases of both the spectra and the photometry. Therefore, our maps show the position of the surface features in the reference frame of the binary motion where zero phase is a time of quadrature with the primary receding.

3.2. Results

The Doppler imaging results are summarized in Fig. 2. The "average" maps are plotted as pseudo-Mercator (cylindrical equidistant) projections and as polar-mesh projections for each season from 1994 through 2000. The supporting light curves and their fits as well as the Ca I 6439-Å line profiles and their fits are also shown in Fig. 2. "Average" maps are made up from the individual maps from the three different wavelength regions without a particular weighting. The reason for doing so is that surface features that are present in the maps from all three wavelength regions are most likely real, and thus appear emphasized in the average map. However, the inconsistencies in the temperature determination are also levelled up when we sum up the individual maps, so the precision increases but not the accuracy. The number of spectra per map varies between 8 and 12, but were taken always within about two stellar rotations (cf. Table 1). The basic spot distribution appears to be stable during such a short time interval, as shown just recently by Oláh et al. (2002a) for a much longer time interval of continuous photometry. The solid-line contours on the pseudo-Mercator maps in Figs. 2a–h enclose regions cooler than 4500 K, i.e. 300 K below the effective temperature. This value closely resembles the empirical temperature threshold due to the

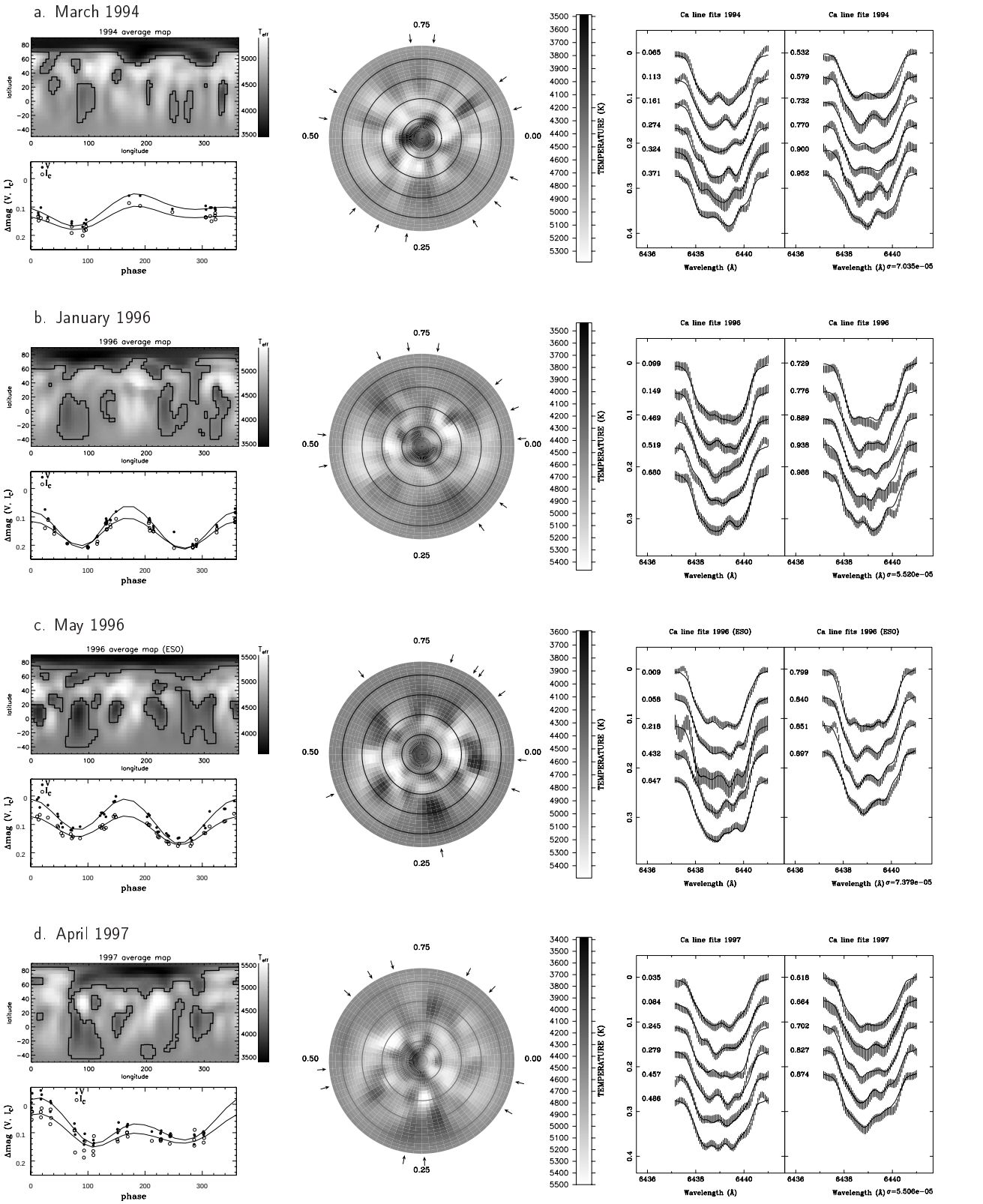

Fig. 2. Average Doppler maps of UZ Lib for 1994–2000. The contours in the pseudo-Mercator maps represent isothermal lines at 4500 K, separating regions cooler by 300 K relative to the unspotted photosphere. The photometric data is plotted below each pseudo-Mercator map as symbols along with the averaged fits (again resulting from the individual maps from the different spectral regions). A polar-mesh projection of the average maps, but without contours, is shown in the middle panels. The arrows mark the phases of the spectra. The Ca I line profiles and their fits are plotted in the right-side panel. The intensity per wavelength bin is represented as a ± 1-σ bar proportional to the reciprocal S/N ratio.

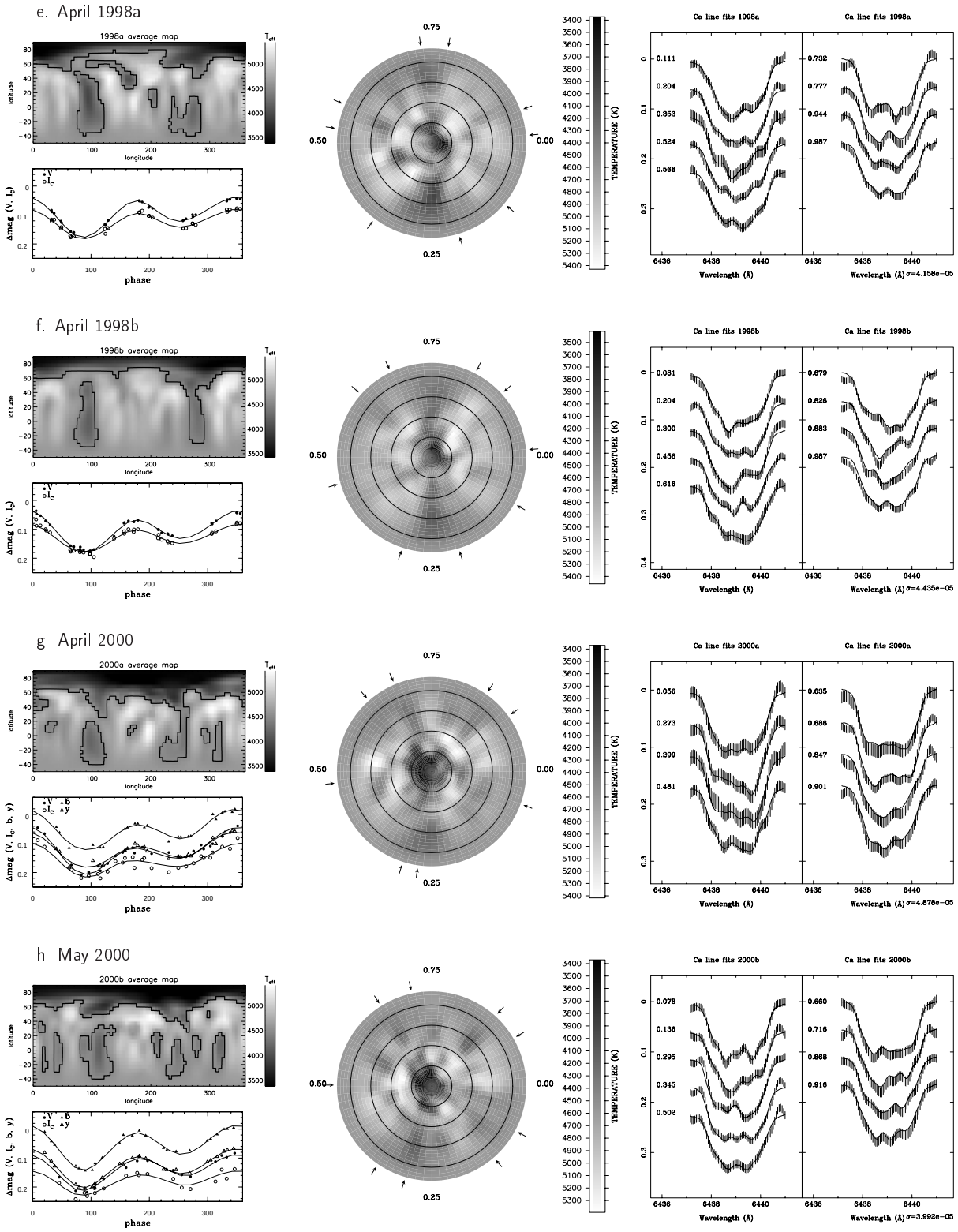

Fig. 2. continued.

moderate S/N ratio of the spectra combined with the relatively large line broadening. We consider the recovery of the encircled regions to be significant. These regions concentrate close to and at the visible rotational pole as well as along the stellar equator at longitudes of roughly 90° and 270°. This pattern persists over the seven years of our spectroscopic observations with some local changes within the equatorial regions and along the rim of the polar spot.

The map for 1994 is practically identical to the one derived by Strassmeier (1996) from the same data but with a very early version of TempMap. He used an inclination of $i = 30°$ but remarked that the resulting maps were nearly

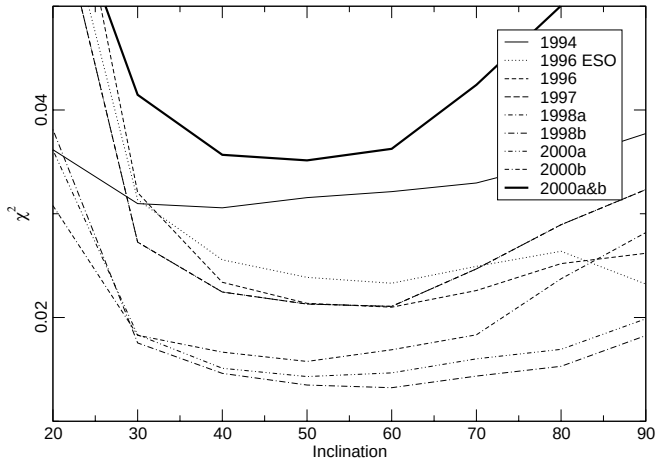

Fig. 3. The misfit between the data and the predicted line profiles and light curves (χ^2) as a function of the inclination of the stellar rotational axis. The most probable range of the correct inclination is between 35° and 65° with a preference of an inclination of near $50° \pm 10°$. Note that Strassmeier (1996) had preferred $i = 30°$ from the 1994 data alone.

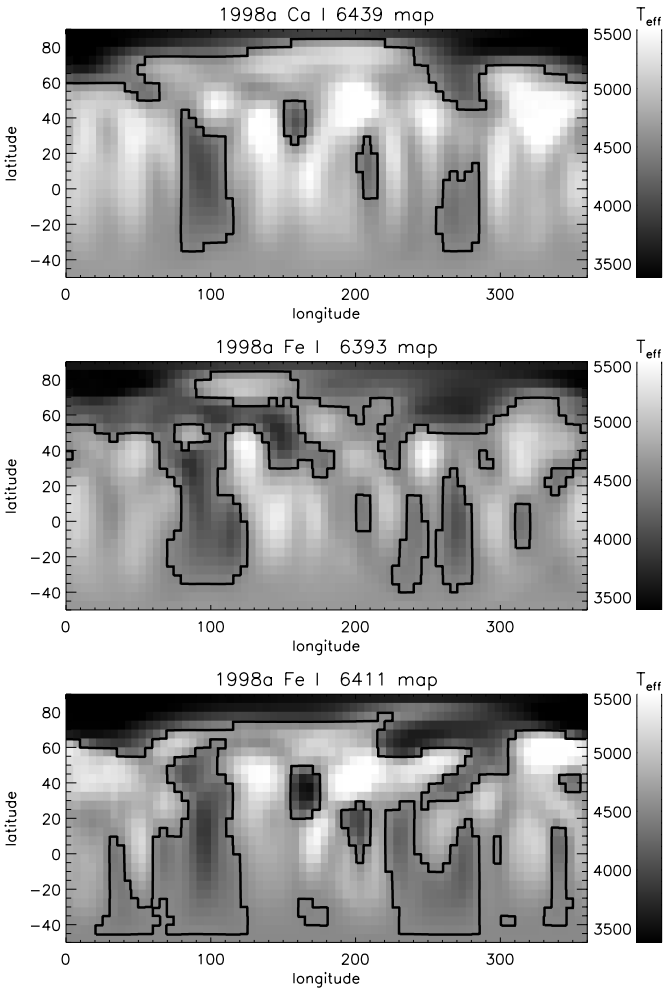

Fig. 4. Individual line maps from the 1998a data set: the Ca I map (top), the Fe I-6393 map (middle) and the Fe I-6411 map (bottom). The contours represent 4500 K, marking 300-K cooler regions relative to the photosphere. It is well seen that the iron maps show more surface details than the calcium map. The average from these three maps is shown in Fig. 2e.

the same for inclinations between 25°–60°. In the present paper, we quantify this statement by plotting the discrepancy integral from the TempMap output – a (pseudo) χ^2 value for each set of spectra and light curve fits – versus the inclination of the stellar rotational axis (see also, e.g., Rice & Strassmeier 2000; Weber & Strassmeier 2001; Kővári et al. 2001). Note that throughout this paper a relative weight of 0.3 was assigned to the photometry as compared to the line profiles. Figure 3 shows the change of the misfit for inclinations from 20° to 90° for all eight data sets, and for the combination of the two datasets from 2000. The range of equally likely inclinations is between 35° and 65° with a preference of an inclination of near $50° \pm 10°$, that is the most likely using the combined 2000 dataset. This is also the inclination we adopted.

The spots on UZ Lib are 300–1300 K cooler than the photosphere. The equatorial spots appear generally warmer (≈4000–4500 K) than most of the polar spot (≈3500–3800 K). We obtain a pseudo effective temperature of 4670 K from the grand average Doppler map (shown later in Fig. 9) and compare it to the value obtained from the multi-color photometry alone (4700 K, Oláh et al. 2002a). The good agreement of the two results means that the general surface-temperature deficiency due to the cool spots is reasonably well determined.

We have two maps for 1996 taken about 25 rotations (120 days) apart in January and May (Figs. 2b and c). The May set of these observations is the only one obtained at ESO with significantly higher spectral resolution. Due to the smaller wavelength coverage of these spectra only the Ca I 6439 Å and the Fe I 6411 Å lines could be used for mapping. Despite a $0\overset{m}{.}08$ brightening of the maximum V magnitude from January 1996 to May 1996, an additional cool feature appears near the equator at a longitude of ≈0° and seems to be a freshly emerged spot. Its temperature difference appears larger by 300 K from the iron line than from the calcium line which is a little bit suspicious. However, the following map in April 1997 (Fig. 2d), observed at the highest system brightness detected so far, possibly shows a remnant of this feature, making it more believable. In this map it is also well seen that the polar feature is smaller than before but the size of the equatorial spots remained similar to the ones during the other epochs. This suggests that the polar spot is the cause of the overall light variations of the system (compare with Fig. 1). The two consecutive maps in April 1998 (Figs. 2e and f) show basically a stable spot distribution but with some features becoming warmer by up to 300 K by the end of April. The two maps in April and May 2000 (Figs. 2g and h) are separated by approximately five stellar rotations and show a more deviant appearance, mostly in the form of a segregation of the two main equatorial spotted regions into smaller spots by May 2000. Additionally, the coolest part of the asymmetric polar cap had shifted to a

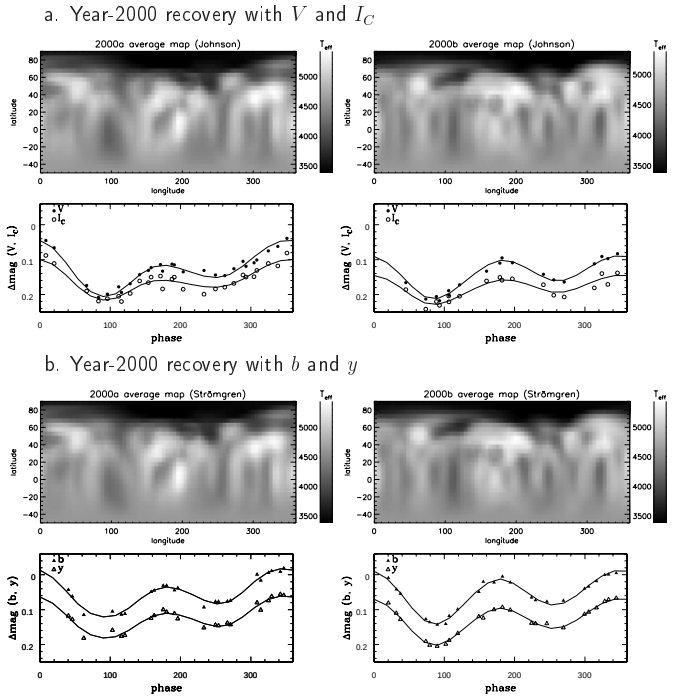

Fig. 5. A comparison of Doppler maps for the data set April 2000 (left column) and May 2000 (right column) using **a)** Johnson and **b)** Strömgren photometry. Note the deviant I_C curve due to the higher flux contribution from the cool regions but the more or less identical recovery of its surface structure.

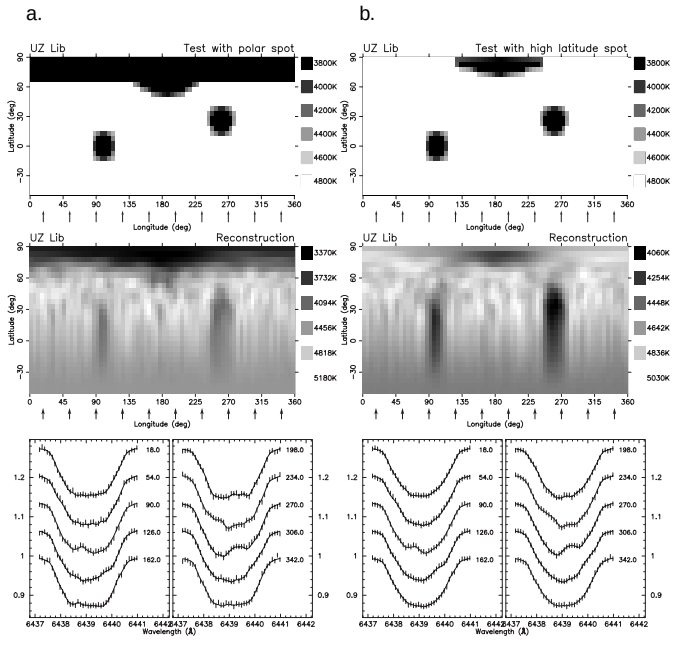

Fig. 6. Tests for checking the reality of appendages of the polar spots recovered on UZ Lib. **a)** The input image with a polar spot (top), the reconstruction with S/N 200 (middle), and the artificial spectra (bottom). **b)** The same with a high latitude but not exactly polar spot.

longitude of around 200° by April 2000 (as compared to around 0° in April 1998).

3.3. Consistency checks

Figure 4 is a check of the consistent recovery from different wavelength regions and shows indeed that the resulting maps of the different spectral lines contain the same or similar surface structure. The Ca I-6439 line is stronger and more temperature sensitive than the iron lines and thus its inversion shows less detail than the iron maps, as noticed and discussed in several previous papers (e.g. by Vogt et al. 1987; Strassmeier & Bartus 2000 and Collier Cameron & Unruh 1994).

For the two data sets in 2000, we have contemporaneous and simultaneous Johnson V, I_C and Strömgren b, y photometry from the two Vienna APTs in Arizona. These four bandpasses cover a wide range of wavelengths, from 487 nm for b to 787.5 nm for I_C (Strassmeier et al. 1997b), thereby sampling the flux contribution from the (cool) spotted regions which should be highest in the red wavelengths. Therefore, we attempt to recover the two year-2000 images with either blue and yellow and yellow and red bandpass photometry. There is practically no difference in the recovered maps in Fig. 5. Nevertheless, note the deviant light curve shape of the I_C curve – and its fit – as compared to the other bandpasses which implies, more or less obviously, that the $V - I_C$ color is treated correctly by the inversion code.

3.4. An old debate: How "real" is all of this?

Tests were performed to check whether the appendages to the polar spots are real or just artifacts due to the low latitude features that are present in all images. We placed two low latitude spots at $\ell = 100°$, $b = 0°$ and $\ell = 260°$, $b = +25°$ (Fig. 6). Additionally, we added a polar feature for the first test, and a high latitude ($\ell = 190°$, $b = 80°$) spot for the second test. Noise was added to the resulting artificial spectral lines at the wavelength of Ca I 6439.076 Å to get $S/N = 200$, similar to the S/N ratios of our spectra. The resolution was ≈34 000, again similar to the observations. This way we mimicked our observed spectra and the basic recovered spot pattern. The artificial spectra were then treated exactly as the observed ones, using the same parameters and blends. The result is depicted in Fig. 6. No definite appendages were found as artifacts close or attached to the polar or high latitude features. Although we cannot exclude the possibility that some artifact appendages may appear (see, e.g., the tests in Rice & Strassmeier 2000, their Fig. 2, Case 1, at $S/N = 150$), but we believe that most of the recovered high latitude features on UZ Lib are real.

A second "test" was performed by using only photometric data. We separated the photometry from the Doppler imaging analysis and performed an independent spot-modelling analysis on all of them. The latter is a simultaneous fit of the light and color curves under the assumption of no more than three circular spots of uniform and equal temperature. The technical details of this approach, together with its application to a total of

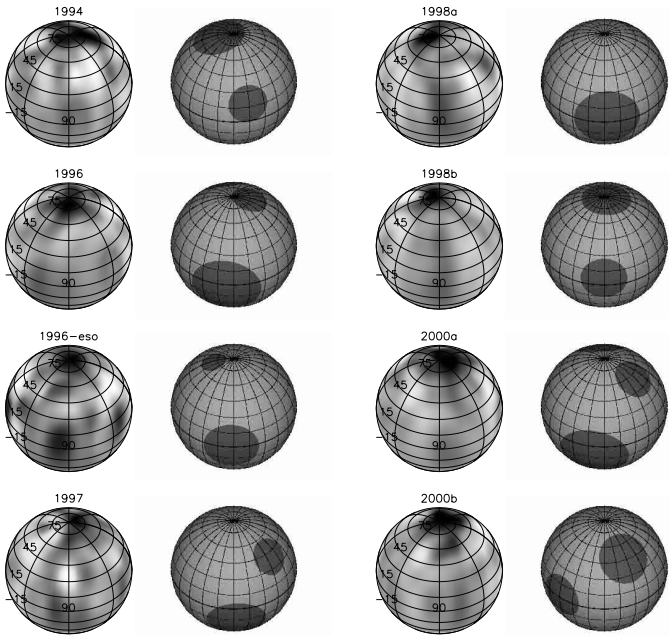

Fig. 7. A comparison of the Doppler maps from Fig. 2 with purely photometric maps for the years 1994 to 2000 (the photometric maps are the ones with the circular spots, see text).

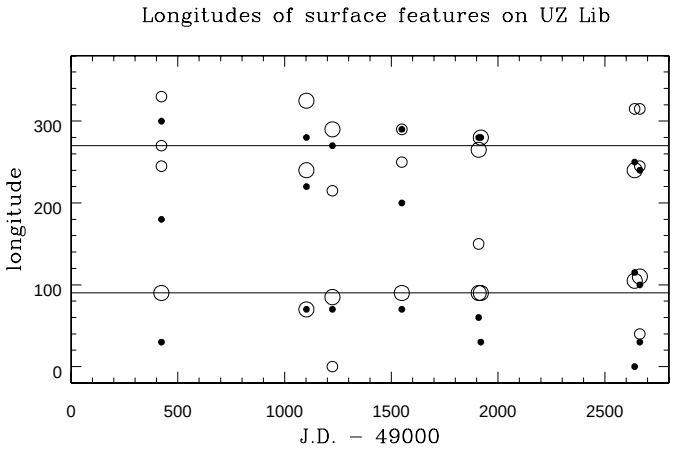

Fig. 8. The distribution of spot longitudes from 1994 through 2000. Plotted are the longitudes of the polar-spot appendages (filled dots) and of the most significant equatorial spots weighted by their size (larger and smaller open circles for large and medium-sized spots, respectively). The horizontal lines near 90° and 270° represent the weighted-average longitudes of the equatorial spots that we interpret to be "preferred" longitudes of spot emergence.

40 light curves, is published in a separate paper (Oláh et al. 2002a). For the present comparison, we use the same eight contemporaneous and simultaneous photometric data sets already employed for the Doppler images. This gives us the ability to directly compare the two techniques and thus better access their model-dependency and thus their reality. The comparison is shown in Fig. 7. The results from the photometric spot modelling are comparably unstable because of the limited information content due to the one-dimensional data and the large number of free parameters. The Doppler-imaging technique imposes much greater constraints due to the (pseudo) two-dimensional information in the resolved line profiles, plus the additional supporting photometry. Thus, the Doppler maps are much more reliable than the simplified photometric models with circular spots. Nevertheless, the comparison in Fig. 7 is still quite good, at least for the larger features. The photometric approach clearly suffers from the well-known deficiency of latitude resolution, which may cause a spurious spot distribution, e.g. for the May-2000 data (the 2000b set in Fig. 7), but in general support the Doppler maps.

4. Discussion

4.1. Preferred spot positions? Yes

Visual inspection of the time sequence of maps in Fig. 2 already suggests two preferred longitudes at around 90° and 270°. With a few exceptions, the appendages of the polar spot also appear close to these two preferred locations, and sometimes seem to be connected to them. Figure 8 is a plot of the recovered longitudes for the most significant surface features versus time. For this plot, longitudes were estimated by eye from the 4500-K contours off the maps in Fig. 2 (we found this a more consistent procedure than, e.g., numerically identifying the coolest n pixels within a given feature and then interpolating). Figure 8 quantifies the two preferred longitudes from such a visual inspection by simply calculating a weighted average, where the weight is chosen proportional to the size of the feature. The most likely longitudes are $86° \pm 33°$ (rms) and $274° \pm 34°$ (rms), respectively.

Another possibility to find preferred surface positions is to combine all available Doppler maps into a single "grand average map" for the seven years from 1994–2000. Any persistent spot morphology must then also appear in this map or, to falsify such an assumption, a random spot distribution must result in a smeared grand map and leaves no or only little structure. The grand map in Fig. 9 clearly shows a recognizable pattern similar to the annual average images in Fig. 2. It thus verifies the existence of preferred longitudes and latitudes. The darkest region, i.e. the region with the highest likelihood of finding a spot, is the polar region down to a latitude of about +60°. The two main equatorial regions, slightly less significant than the polar region, appear as well and are facing the (unseen) companion star at 90° and opposite to it at 270°. It seems that the facing hemisphere is even more preferred than the anti-facing region. Two appendages of the polar spot appear closely related to the two equatorial active regions. The first appendage slightly precedes the 90°-region, the second possibly succeeds the 270°-region. The second panel in Fig. 9 shows the surface distribution of the standard deviations in Kelvin. The scatter is mostly below ±200 K with some exceptions of up to ±300 K, but still of the same order as the image threshold due to the limited quality of the spectra.

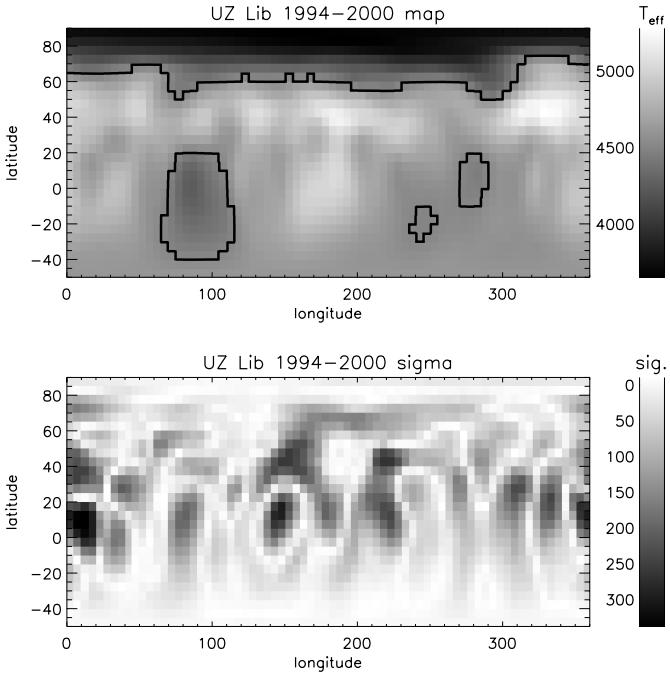

Fig. 9. The "grand average Doppler map" for 1994–2000 (top) and its standard-deviation map in Kelvin (bottom). Dark regions mark the highest likelihood of finding a spot. Again, contours are drawn at temperatures of 4500 K.

A spot distribution comparable to UZ Lib was found for many spotted stars in binary systems, e.g. on the active giant DM UMa in 1993 (Hatzes 1995), on the two main-sequence components of σ^2 CrB in 2000 (Strassmeier & Rice 2002) or on the two pre-main-sequence components of V824 Ara in 1990 (Hatzes & Kürster 1999) and in 1996 (Strassmeier & Rice 2000). On that star, the equatorial spots appeared preferentially on the anti-facing hemispheres while the polar appendages either faced each other (in 1996) or anti-faced each other (in 1990). Even simple mean-field dynamo theory applied to two active stars in a binary system suggests a large variety of non-axisymmetric magnetic fields (Moss & Tuominen 1997). These may be of even parity if the components are detached and the visible fields then have maxima at the longitudes corresponding to the intersection of the apsidal line with the stellar surfaces.

From photometry alone, various authors repeatedly claimed a similar picture for a handful of objects, including UZ Lib, e.g. by the series of papers by Zeilik et al. (1990), Henry et al. (1995), Jetsu (1996), Berdyugina & Tuominen (1998), and for UZ Lib by Oláh et al. (2002a). Evidence is now growing that preferred longitudes also exist on active *single* stars, e.g. on the G-giant FK Comae from several years of Doppler imaging and photometry (Korhonen et al. 2001; see also Jetsu et al. 1994) or on the weak-line T Tauri star V410 Tau (Rice & Strassmeier 1996; Granzer et al. 2001). Binarity may favor preferred longitudes though, but likely just causes this same effect that is of different physical origin (at last there is evidence for some non-axisymmetric large-scale features on the Sun as well; Jetsu et al. 1997). Further progress is now expected from time-series spectro-polarimetric Doppler imaging (e.g. Kitchatinov et al. 2000; Donati 1999).

4.2. Differential rotation detected? No

Tidal interaction between two stellar components is thought to suppress surface differential rotation (Schrijver & Zwaan 1991; Moss & Tuominen 1997) while the asymmetric heating of the convective layer due to a tidally deformed star should stimulate differential rotation and meridional circulation (Rüdiger & Küker 2002). In any case, there is substantial theoretical arguments for and against large-scale surface flows but only few conclusive observations.

With our UZ Lib observations in 1998 and 2000, we have two closely spaced sets of data in each year that we may use to detect a coherent differential-rotation (or meridional-flow) pattern. The two maps in 1998 were basically back to back in time, we even used two overlapping spectra taken on two consecutive nights, whereas for the maps in 2000 there were five stellar rotations in between. We cross correlate the two respective maps according to the recipe layed out in an earlier paper (e.g. in Weber & Strassmeier 2001) and based on an idea by Donati & Collier Cameron (1997). The results are shown in Fig. 10. The cross correlations from the Ca I and the Fe I 6393 Å maps appear very similar while the cross correlations from the Fe I 6411 maps deviate in some (mostly high latitude) details but agree with the other ones on average. All of them show no systematic deviation until up to a latitude of around $+50°$, i.e. for the latitudes where the cross-correlation signal is well defined. Our result for the lower latitudes is not conclusive and means that, if differential rotation is present at all, it has a much smaller scale than on the Sun or on other single stars. According to our previous experience (e.g. Weber & Strassmeier 2001) we can detect a longitudinal shift of $0.2°$/day at the 1-σ level in the case of a $\sin^2 b$ fit leads to an acceptable rms. Thus, for UZ Lib, the differential rotation parameter $\alpha(\equiv\Delta\Omega_{\rm pole-eq}/\Omega_{\rm eq})$ is smaller than $\approx$0.04, i.e. about five times weaker than on the Sun. In the case of a "non-solar" longitudinal shift pattern, we estimate a detection threshold of at least twice that value for the peak shift.

A systematic shift towards larger longitudes appears for the near-polar regions. If real, this must be caused by the various appendages of the polar spots that seem to indicate an acceleration as compared to the equatorial features. The effect appears in both years but is more pronounced in 2000, most likely because there is a time gap between the two maps. We must stress, however, that the high latitude features are less well defined, and some detail maybe spurious. Thus, whether the above mentioned acceleration is due to non-solar differential rotation or is a chance alignment remains to be determined. Note that in Fig. 10 the correlation along the $\pm180°$-longitude shifts

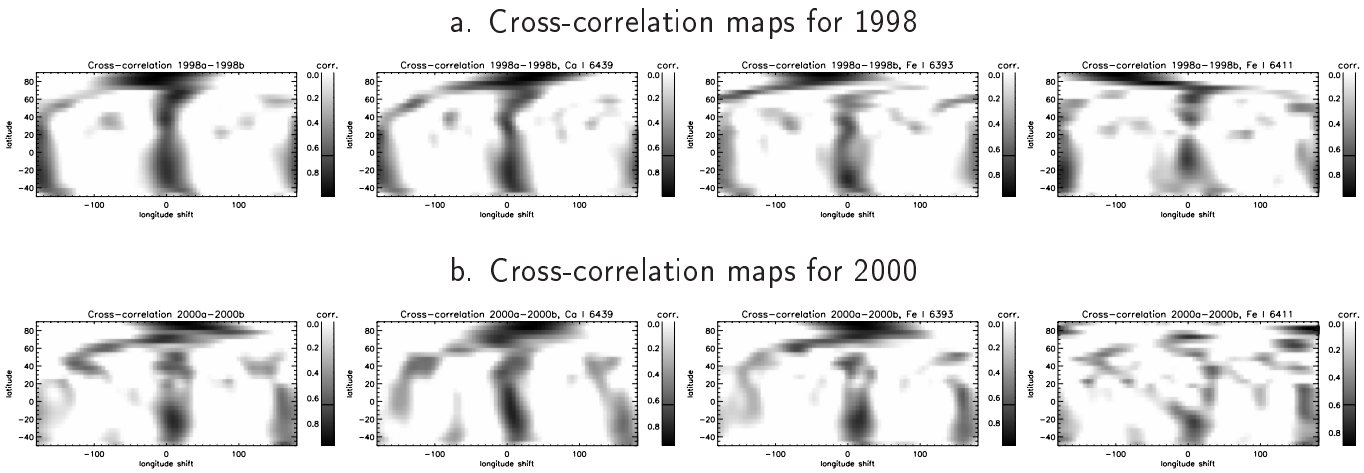

Fig. 10. Cross-correlation maps for the years **a)** 1998 and **b)** 2000. From left to right: cross correlation of the average maps, the Ca I-6439 maps, the Fe I-6393 maps, and the Fe I-6411 maps.

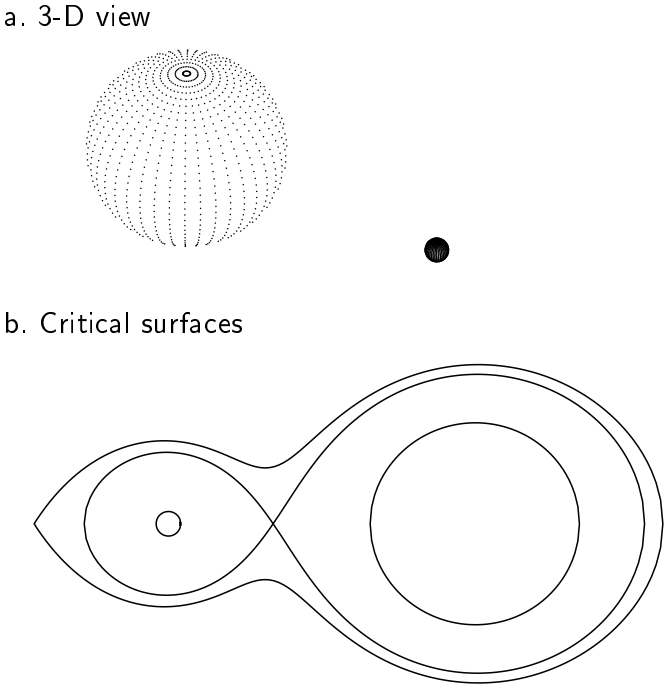

Fig. 11. The binary scenario for UZ Lib. **a)** A hypothetical view of the binary system at phase 0.16 with $i = 50^\circ$ and $m_2/m_1 = 0.3$. **b)** Critical Roche equipotentials. Shown are the inner and the outer equipotentials and the stellar surfaces.

are a natural consequence of the symmetric spot grouping on opposite hemispheres of the star.

4.3. Absolute dimensions

The Hipparcos parallax revised the distance to UZ Lib from keen 550 pc (Grewing et al. 1989) and 450 pc (Strassmeier 1996) to a mere 140 ± 22 pc. Given the photometric properties, this suggests a radius of UZ Lib of $3.4 \pm 0.7\ R_\odot$, in outraging disagreement with the minimum radius of $6.28 \pm 0.07\ R_\odot$ from $v_{\rm rot} \sin i$ and $P_{\rm rot}$ (Fekel et al. 1999). Our best value of the inclination of $i = 50^\circ$ even worsens the disagreement, yielding $R \approx 8.2\ R_\odot$. A discrepancy of similar amount is found for the active binary HD 106225 (HU Vir) that later was discovered to be a spectroscopic triple system by Fekel et al. (1999). Furthermore, a close match of the activity phenomenology seems to exist with another triple system: IN Comae (Strassmeier et al. 1997c), an active G5 giant in a close single-lined orbit with an unseen companion and a very hot O subdwarf as the third component (its G5 primary also shows a stable light-curve minimum indicative of a preferred spot longitude). We thus tentatively imagine three scenarios that could resolve the radius disagreement for UZ Librae. Firstly, UZ Librae could be an undiscovered triple system and the Hipparcos parallax thus incorrect by, say, a factor of two or, secondly, the rotation period is not equal to the orbital period but only one half of it (which we can safely exclude due to the then abstract light curves) or, thirdly, all previous $v \sin i$ measures are wrong by a factor of two due to an unknown reason (an ellipticity effect or a bizarre differential surface rotation would not be sufficient to cause a factor of two). This leaves little choice other than erroneous Hipparcos parallax.

It is worth mentioning the results of Szabados (1997), who found that the Hipparcos parallaxes were strongly influenced by the orbital motion of binary Cepheids, and lists 7 cases with known orbital period and $a \sin i$ values. Among those binaries e.g. FF Aql ($P_{\rm orb} = 1429.7$ days) has the same $a \sin i$ value as HU Vir ($P_{\rm orb} = 2226.6$ days, Fekel et al. 1999). Moreover, Szabados (1997) found, that the binary motion is also reflected in the relative accuracy of the parallax data of Hipparcos.

We thus favor a binary scenario as sketched in Fig. 11. Then, UZ Lib is a K0 giant, has a low-mass secondary instead of a hot secondary (as claimed by Grewing et al. 1989), a mass ratio of $m_2/m_1 \leq 0.3$ in order to match $i \approx 50^\circ$, and the ultraviolet excess is explained by its very active chromosphere (and not by a hot secondary).

5. Summary and conclusions

- We obtained eight Doppler images for the years 1994 through 2000 from a total of 68 medium-resolution spectra and 237 VI_C and 47 *by* data points. No map included data from more than two consecutive stellar rotations.
- The general morphology of the spot pattern on the surface of UZ Lib remains persistent from 1994 to 2000. It consists of a cool polar spot and two less cool equatorial spot concentrations at around longitudes of $86° \pm 33°$ and $274° \pm 34°$ (rms). The polar spot is variable in size and dominates the overall system brightness.
- The cross-correlation functions of two closely-spaced maps in 1998 and 2000 show a null shift for latitudes up to approximately $+50°$. Latitudes above $50°$ may show a systematic shift indicating acceleration compared to the lower latitudes. However, there is no simple interpretation with a solar-like differential-rotation law and the best we can say is that, if the signature is real at all, UZ Lib exhibits a non-solar flow pattern.
- The big-leg-Emma-dilemma of Strassmeier (1996) worsens due to the surprisingly large Hipparcos parallax!

Acknowledgements. The authors are grateful to the referee, Dr. John Barnes, whose advices helped us to improve the paper. KO wishes to thank Dr. Zs. Kővári for his continuous collaboration, Drs. J. Bartus and R. Vavrek for their valuable help in some technical issues of this work, and acknowledges financial support from the Hungarian government through OTKA T-032846 and T-038013, and from the Hungarian-French Intergovernmental grant F-11/99. KGS and MW appreciate support from the Deutsche Forschungsgemeinschaft (DFG) through project STR645/1-1 and HU532/8 and from the Austrian Science Foundation (FWF) grant S7301-AST and S7302-AST during an earlier stage of this project. KO was supported by the Hungarian-German intergovernmental grant D21-01.

References

Berdyugina, S. V., & Tuominen, I. 1998, A&A, 336, 25
Bopp, B. W., & Stencel, R. R. 1981, ApJ, 247, L134
Collier Cameron, A., & Unruh, Y. C. 1994, MNRAS, 269, 814
Donati, J.-F. 1999, MNRAS, 302, 457
Donati, J.-F., & Collier Cameron, A. 1997, MNRAS, 291, 1
Fekel, F. C., Strassmeier, K. G., Weber, M., & Washuettl, A. 1999, A&AS, 137, 369
Granzer, T., Reegen, P., & Strassmeier, K. G. 2001, AN, 322, 325
Grewing, M., Bianchi, L., & Garrido, R. 1989, A&A, 223, 172
Hatzes, A. P. 1995, AJ, 109, 350
Hatzes, A. P., & Kürster, M. 1999, A&A, 346, 432
Henry, G. W., Eaton, J. A., Hamer, J., & Hall, D. S. 1995, ApJS, 97, 513
Jetsu, L. 1996, A&A, 314, 153
Jetsu, L., Pohjolainen, S., Pelt, J., & Tuominen, I. 1997, A&A, 318, 293
Jetsu, L., Tuominen, I., Grankin, K. N., Mel'Nikov, S. Yu., & Schevchenko, V. S. 1994, A&A, 282, 9
Kitchatinov, L. L., Jardine, M., & Donati, J.-F. 2000, MNRAS, 318, 1171
Korhonen, H., Berdyugina, S. V., Strassmeier, K. G., & Tuominen, I. 2001, A&A 379, 30
Kővári, Zs., Strassmeier, K. G., Bartus, J., et al. 2001, A&A, 373, 199
Kurucz, R. L. 1993, ATLAS-9, CD-ROM, No. 13.
Moss, D., & Tuominen, I. 1997, A&A, 321, 151
Oláh, K., Strassmeier, K. G., & Granzer, T. 2002a, AN, submitted
Oláh, K., Strassmeier, K. G., & Weber, M. 2002b, Proc. 12th Cool Stars, Stellar Systems and the Sun (Cambridge, USA), in press
Piskunov, N. E., & Rice, J. B. 1993, PASP, 105, 1415
Rice, J. B., & Strassmeier, K. G. 1996, A&A, 316, 164
Rice, J. B., & Strassmeier, K. G. 2000, A&AS, 147, 151
Rice, J. B., & Strassmeier, K. G. 2001, A&A, 377, 264
Rice, J. B., Wehlau, W. H., & Khokhlova, V. L. 1989, A&A, 208, 179
Rüdiger, G., & Küker, M. 2002, A&A, submitted
Schrijver, K., & Zwaan, C. 1991, A&A, 251, 183
Stempels, H. C., Piskunov, N. E., & Barklem, P. S. 2001, in Cool Stars, Stellar Systems, and the Sun, 11th Cambridge Cool Star Workshop, ed. R. Garcia Lopez, R. Rebolo, & M. R. Zapaterio Osorio, PASPC 223, CD-ROM, 878
Strassmeier, K. G. 1996, A&A, 314, 558 (Paper I)
Strassmeier, K. G., & Bartus, J. 2000, A&A, 354, 537
Strassmeier, K. G., Bartus, J., Cutispoto, G., & Rodonó, M. 1997a, A&AS, 125, 11
Strassmeier, K. G., Boyd, L. J., Epand, D. H., & Granzer, T. 1997b, PASP, 109, 697
Strassmeier, K. G., Hubl, B., & Rice, J. B. 1997c, A&A, 322, 511
Strassmeier, K. G., & Rice, J. B. 2000, A&A, 360, 1019
Strassmeier, K. G., & Rice, J. B. 2002, A&A, in preparation
Strassmeier, K. G., Serkowitsch, E., & Granzer, T. 1999, A&AS, 140, 29
Szabados, L. 1997, in Hipparcos-Venice '97, ESA SP-402, 657
Vogt, S. S., Penrod, G. D., & Hatzes, A. P. 1987, ApJ, 321, 496
Weber, M., & Strassmeier, K. G. 2001, A&A, 373, 974
Zeilik, M., Cox, D. A., Ledlow, M., et al. 1990, ApJ, 363, 647